

Dynamic relationships between age, amyloid- β deposition, and glucose metabolism link to the regional vulnerability to Alzheimer's disease

Hwamee Oh,^{1,*} Cindee Madison,¹ Suzanne Baker,² Gil Rabinovici,^{1,2,3} and William Jagust^{1,2}

Although some brain regions such as precuneus and lateral temporo-parietal cortex have been shown to be more vulnerable to Alzheimer's disease than other areas, a mechanism underlying the differential regional vulnerability to Alzheimer's disease remains to be elucidated. Using fluorodeoxyglucose and Pittsburgh compound B positron emission tomography imaging glucose metabolism and amyloid- β deposition, we tested whether and how life-long changes in glucose metabolism relate to amyloid- β deposition and Alzheimer's disease-related hypometabolism. Nine healthy young adults (age range: 20–30), 96 cognitively normal older adults (age range: 61–96), and 20 patients with Alzheimer's disease (age range: 50–90) were scanned using fluorodeoxyglucose and Pittsburgh compound B positron emission tomography. Among cognitively normal older subjects, 32 were further classified as amyloid-positive, with 64 as amyloid-negative. To assess the contribution of glucose metabolism to the regional vulnerability to amyloid- β deposition, we defined the highest and lowest metabolic regions in young adults and examined differences in amyloid deposition between these regions across groups. Two-way analyses of variance were conducted to assess regional differences in age and amyloid- β -related changes in glucose metabolism. Multiple regressions were applied to examine the association between amyloid- β deposition and regional glucose metabolism. Both region of interest and whole-brain voxelwise analyses were conducted to complement and confirm the results derived from the other approach. Regional differences in glucose metabolism between the highest and lowest metabolism regions defined in young adults ($T = 12.85$, $P < 0.001$) were maintained both in Pittsburgh compound B-negative cognitively normal older subjects ($T = 6.66$, $P < 0.001$) and Pittsburgh compound B-positive cognitively normal older subjects ($T = 10.62$, $P < 0.001$), but, only the Pittsburgh compound B-positive cognitively normal older subjects group showed significantly higher Pittsburgh compound B retention in the highest compared to the lowest glucose metabolism regions defined in young adults ($T = 2.05$, $P < 0.05$). Regional differences in age and amyloid- β -dependent changes in glucose metabolism were found such that frontal glucose metabolism was reduced with age, while glucose metabolism in the precuneus was maintained across the lifespan (right hemisphere: $F = 7.69$, $P < 0.001$; left hemisphere: $F = 8.69$, $P < 0.001$). Greater Alzheimer's disease-related hypometabolism was observed in brain regions that showed both age-invariance and amyloid- β -related increases in glucose metabolism. Our results indicate that although early and life-long regional variation in glucose metabolism relates to the regional vulnerability to amyloid- β accumulation, Alzheimer's disease-related hypometabolism is more specific to brain regions showing age-invariant glucose metabolism and amyloid- β -related hypermetabolism.

1 Helen Wills Neuroscience Institute, University of California-Berkeley, Berkeley, CA 94720, USA

2 Life Sciences Division, Lawrence Berkeley National Laboratory, Berkeley, CA 94720, USA

3 Memory and Aging Center and Department of Neurology, University of California-San Francisco, San Francisco, CA 94117, USA

*Present address: Department of Neurology and Taub Institute, Columbia University College of Physicians and Surgeons, 630 West 168th St, P&S 16, New York, 10032, USA

Correspondence to: Hwamee Oh,
Department of Neurology and Taub Institute,
Columbia University College of Physicians and Surgeons,
630 West 168th St, P&S 16, New York, 10032,
USA
E-mail: hwamee.oh@columbia.edu

Keywords: glucose metabolism; beta-amyloid deposition; regional vulnerability; Alzheimer's disease pathology; cognitively normal older adults

Abbreviations: DMN = default mode network; DVR = distribution volume ratio; PiB = Pittsburgh compound B; PVC = partial volume correction

Introduction

Alzheimer's disease is characterized by pathological markers of tau-protein neurofibrillary tangles and neuritic amyloid- β plaques and is associated with hypometabolism in posterior brain regions that correlates with cognitive impairment in Alzheimer's disease. Recent models of the relationships between Alzheimer's disease biomarkers propose that neuritic amyloid- β plaques may be an early event leading to neurofibrillary tangles, reduced glucose metabolism, brain atrophy, and ultimately dementia (Hardy and Selkoe, 2002; Jack *et al.*, 2010). Consistent with this proposition, PET studies with amyloid binding ligands such as Pittsburgh compound B (PiB) have reported a partially overlapping regional topography between amyloid- β deposition *in vivo* and other neural markers such as hypometabolism (Klunk *et al.*, 2004; Edison *et al.*, 2007; Forster *et al.*, 2012), brain atrophy (Buckner *et al.*, 2005; Jack *et al.*, 2008), and reduced functional connectivity (Sorg *et al.*, 2007) in patients with Alzheimer's disease and mild cognitive impairment. These topographical overlaps are more pronounced in brain regions which are in part considered as the default mode network (DMN) or cortical hubs (Raichle *et al.*, 2001; Greicius *et al.*, 2003; Buckner *et al.*, 2009). The mechanisms underlying regional differences in the vulnerability to amyloid- β deposition and subsequent neurodegenerative changes, however, remain to be elucidated.

A convergence of animal and human studies has suggested that the topographic distribution of amyloid- β accumulation relates to regional differences in steady-state neural activity and physiology early in life before plaque accumulation (Yan *et al.*, 2009; Bero *et al.*, 2011). For example, lactate production indicating neuronal activity was associated with regional concentration of interstitial fluid amyloid- β in young mice, which in turn was related to amyloid- β plaque deposition in the same brain regions in APP transgenic aged mice (Bero *et al.*, 2011), suggesting that long-term regulation of interstitial fluid amyloid- β by neural activity leads to greater amyloid- β plaque accumulation during ageing. In humans, the topography of amyloid- β accumulation overlaps with brain regions showing

aerobic glycolysis (i.e. 10–12% of glucose utilization in excess of that used for oxidative phosphorylation) identified in young adults, indicating a potentially common mechanism underlying amyloid- β accumulation and aerobic glycolysis throughout life (Vaishnavi *et al.*, 2010; Vlassenko *et al.*, 2010). Increased neural activity measured by functional MRI was also observed in brain regions with a higher level of amyloid- β deposition during a task in cognitively normal older adults harbouring elevated amyloid- β deposition (Sperling *et al.*, 2009; Mormino *et al.*, 2012a), although the relationship between amyloid- β deposition and concurrent neural activity could be bidirectional. Taken together, regional variations in long term as well as concurrent neuronal activity might contribute to regional differences in amyloid- β deposition, which in turn could result in metabolic changes reflecting neuronal and synaptic dysfunction.

In addition to links between neural activity and amyloid- β deposition, glucose metabolism as measured by ^{18}F -fluorodeoxyglucose (FDG) PET is also well-documented to change in association with Alzheimer's disease (Mosconi, 2005). In particular, hypometabolism in patients with Alzheimer's disease compared with age-matched control subjects is regionally specific and prominent in lateral temporoparietal, medial parietal, and posterior cingulate cortices (Minoshima *et al.*, 1997; Landau *et al.*, 2011). The mechanism underlying the regional distribution of Alzheimer's disease-related hypometabolism, however, remains unclear. One possibility is that regional glucose metabolism is affected by the deposition of amyloid- β itself, which occurs in cognitively normal older people, presumably on a pathway to frank Alzheimer's disease (Bennett *et al.*, 2006). While some studies have shown amyloid- β -related decreases in glucose metabolism in cognitively normal older adults, several recent studies have shown that cognitively normal older adults with amyloid- β deposition show increased glucose metabolism in brain regions that commonly undergo hypometabolism in patients with Alzheimer's disease (Benzinger *et al.*, 2013; Johnson *et al.*, 2014; Oh *et al.*, 2014; Ossenkoppele *et al.*, 2014). In addition, age itself is associated with metabolic reductions in some brain regions, particularly in prefrontal cortex

(Mielke *et al.*, 1998; Kalpouzos *et al.*, 2009; Knopman *et al.*, 2014), while metabolic rates are maintained in other regions, potentially indicating these regions' constant neural/synaptic activity throughout the lifetime. If the age-related reduction in glucose metabolism precipitates further metabolic disruption in the progression of Alzheimer's disease, brain regions sensitive to age-related metabolic reduction may undergo Alzheimer's disease-related hypometabolism. If age-invariant metabolic utilization eventually leads to a breakdown of the system, however, brain regions showing age-invariance of metabolic usage would show greater Alzheimer's disease-related hypometabolism. While these age and amyloid- β -related changes in glucose utilization during ageing may independently or interactively contribute to the regional differences in Alzheimer's disease-related hypometabolism, a systematic investigation of metabolism changes across the whole brain along the continuum of ageing and amyloid- β pathology has been lacking. Understanding how age and amyloid- β deposition might affect glucose metabolism in asymptomatic, cognitively normal older people will provide insights into the mechanisms underlying regional metabolic vulnerability in Alzheimer's disease.

In this study, we sought to examine possible mechanisms underlying regional differences in vulnerability to amyloid- β deposition and hypometabolism during the progression to Alzheimer's disease. While both animal and human studies have supported a proposal that brain regions with higher metabolism in youth could be the target for a progressive neurodegenerative cascade initiated by amyloid- β (Buckner *et al.*, 2005; Vlassenko *et al.*, 2010; Bero *et al.*, 2011), direct evidence linking the total amount of glucose metabolism and amyloid- β deposition has been lacking in human studies. In addition, given the known anatomical distribution of amyloid- β deposition, the mechanism underlying regional discordance between amyloid- β deposition and hypometabolism in Alzheimer's disease remains to be elucidated. Using FDG-PET, PiB-PET, and structural MRI, we imaged healthy young people, cognitively normal older adults with and without amyloid- β deposition, and patients with Alzheimer's disease to determine: (i) whether regional differences in synaptic activity measured by FDG-PET in young adults are related to regional topography of amyloid- β deposition in older people; and (ii) whether and how regional differences in age and amyloid- β -related changes in glucose metabolism relate to regional vulnerability to hypometabolism in Alzheimer's disease. We hypothesized that brain regions that show higher glucose metabolism in early life accumulate more amyloid- β during ageing, particularly in the early stage of amyloid- β deposition as demonstrated by cognitively normal older adults harbouring amyloid- β . In addition, we hypothesized that regions showing age-invariant but amyloid- β -related increased metabolism would undergo greater hypometabolism in patients with Alzheimer's disease.

Materials and methods

Participants

Nine healthy young adults (mean age = 24.9 years, four females), 96 cognitively normal older adults (mean age = 74.1 years, 59 females), and 20 patients with Alzheimer's disease (mean age = 68.5 years, 12 females) participated in the study (Table 1). Young and cognitively normal older adults were enrolled in the Berkeley Aging Cohort Study between 2005 and 2013 during which the PET data were collected using the same scanner. The PET data from a subset of cognitively normal older adults were reported in our previous reports (Oh *et al.*, 2014; Ossenkoppele *et al.*, 2014). Cognitively normal older adults were classified as PiB-positive (PiB+ OLD) if their whole-brain PiB uptake [or PiB index measured using a distribution volume ratio (DVR); detailed methods are described below] was greater than 2 standard deviations (SD) above the mean of a group of young adults as described in a previous report (Mormino *et al.*, 2012b). Thirty-two older subjects fell above this threshold of 1.08 and were classified as PiB+ with 64 as PiB-.

All subjects completed PiB-PET, FDG-PET, and structural MRI scans and underwent a medical interview and a detailed battery of neuropsychological tests. Young and cognitively normal older adults were recruited from the community via newspaper advertisement and patients with Alzheimer's disease were a subgroup of patients recruited from the Memory and Aging Center at University of California, San Francisco (UCSF) during the same period as cognitively normal subjects. To be eligible for the study, cognitively normal older subjects were required to be 60 years or older, live independently in the community without neurological or psychiatric illness, and have no major medical illness or medication that influence cognition. All subjects provided informed consent in accordance with the Institutional Review Boards of the University of California, Berkeley, UCSF, and the Lawrence Berkeley National Laboratory (LBNL) prior to their participation.

Neuropsychological cognitive measures

All young and cognitively normal older subjects underwent a detailed battery of neuropsychological tests that encompass multiple cognitive domains, which are described in detail elsewhere (Oh *et al.*, 2012).

Imaging data acquisition

Pittsburgh compound B positron emission tomography

[N-methyl- ^{11}C]-2-(4'-methylaminophenyl)-6-hydroxybenzothiazole (^{11}C -PiB)] was synthesized at LBNL's Biomedical Isotope Facility using a previously published protocol (Mathis *et al.*, 2003). All PET scans were performed at LBNL using a Siemens ECAT EXACT HR PET scanner in 3D acquisition mode. Approximately 15 mCi of ^{11}C -PiB was injected as a bolus into an antecubital vein. Dynamic acquisition frames were obtained over 90 min right after the injection.

Table 1 Characteristics of participants

	Young	PiB- OLD	PiB+ OLD ^a	Alzheimer's disease
<i>n</i>	9	64	32	20
Age, years	24.9 ± 3.6 (20–30)	74.1 ± 5.7 (61–88)	75.5 ± 7.3 (61–96)	68.5 ± 10.6 (50–90)
Education, years	16.0 ± 2.1 (14–20)	17.1 ± 1.9 (12–20)	16.8 ± 1.7 (13–20)	16.9 ± 2.7 (9–22)
Gender, <i>n</i> , F/M ^b	5/4	40/24	19/13	12/8
PiB index	1.02 ± 0.03 (1–1.07)	1.01 ± 0.05(0.8–1.07)	1.29 ± 0.22(1.08–1.8)	1.63 ± 0.15 (1.3–1.9)
APOE-ε4, <i>n</i> (%) ^c	5 (62.5%)	13 (22.6%)	15 (46.9%)	10 (58.8%)
MMSE	28.6 ± 1.5 (26–30)	29.0 ± 1.2 (25–30)	28.7 ± 1.4 (25–30)	21 ± 6.7(1–29)

Values are presented as mean ± SD (range). MMSE = Mini-Mental State Examination.

^aClassified as PiB+ if PiB index was greater than mean + 2 SD of the PiB index of young adults. The resulting cut-off score was 1.08.

^b $\chi^2 = 0.5$, $P > 0.9$.

^cProportion of individuals with APOE genotypes ε3/4 or ε4/4, $\chi^2 = 14.4$, $P = 0.0$.

Fluorodeoxyglucose positron emission tomography

¹⁸F-FDG was purchased from a commercial vendor (IBA Molecular). At a minimum of 2 h after ¹¹C-PiB injection, subjects were injected with 6 to 10 mCi of ¹⁸F-FDG. Six emission frames of 5 min each were acquired starting 30 min after tracer injection, with the subject with eyes and ears unoccluded during tracer uptake.

For both PiB-PET and FDG-PET, 10-min transmission scans for attenuation correction were obtained either immediately prior to or following each ¹¹C-PiB and ¹⁸F-FDG scan. PET data were reconstructed using an ordered subset expectation maximization algorithm with weighted attenuation. Images were smoothed with a 4 mm Gaussian kernel with scatter correction.

Structural MRI

High-resolution structural MRI scans were collected at LBNL on a 1.5 T Magnetom Avanto system (Siemens Inc.) with a 12 channel head coil run in triple mode. One to three high-resolution T₁-weighted magnetization-prepared rapid gradient echo (MPRAGE) scans were collected axially for each subject (repetition time = 2110 ms, echo time = 3.58 ms, flip angle: 15°, field of view = 256 × 256 mm, matrix size: 256 × 256 mm, slices: 160, voxel size = 1 × 1 × 1 mm³).

Imaging data analysis

All PET images were preprocessed using Statistical Parametric Mapping 8 (SPM8; <http://www.fil.ion.ucl.ac.uk/spm/>). A detailed description of the data analysis can be found elsewhere (Oh *et al.*, 2012). Region of interest labelling was implemented using the FreeSurfer v4.4 software package (<http://surfer.nmr.mgh.harvard.edu/>) to create reference regions in the grey matter cerebellum and pons and to perform subsequent region of interest analyses.

Pittsburgh compound B positron emission tomography

The first five PiB frames were summed and all PiB frames including the summed image from one to five frames were realigned to the middle (17th) frame. The subject's structural MRI image was coregistered to realigned PiB frames. PiB DVR was calculated on a voxelwise level using Logan graphical analysis and the subject's grey matter cerebellar reference

region with frames corresponding to 35–90 min post-injection (Logan *et al.*, 1996; Price *et al.*, 2005). DVR images warped to the MNI template were smoothed with an 8-mm full-width at half-maximum Gaussian kernel.

Fluorodeoxyglucose positron emission tomography

Six frames of FDG-PET were realigned using the first frame as a reference and a mean FDG image was generated. The FDG PET mean image was coregistered to the mean PiB PET image, followed by coregistration of the subject's structural MRI image (and associated MRI defined reference regions) to the mean FDG image. This resulted in having FDG and PiB images in the same space for subsequent analysis. The realigned FDG frames were summed across frames and the summed image was intensity normalized on a voxelwise level to the mean value of the pons. Pons-normalized FDG images were warped to an MNI structural template via the subject's MRI and smoothed with an 8-mm full-width at half-maximum Gaussian kernel.

Structural MRI

For all subjects, an averaged single structural T₁ image was processed through FreeSurfer v4.4 to implement region of interest labelling. Details can be found in a previously published report (Oh *et al.*, 2011). Briefly, structural images were bias field corrected, intensity normalized, and skull stripped using a watershed algorithm, followed by a white matter-based segmentation, defining grey/white matter and pial surfaces, and topology correction (Dale *et al.*, 1999; Fischl *et al.*, 2001; Segonne *et al.*, 2004). Subcortical and cortical regions of interest spanning the entire brain were defined in each subject's native space (Fischl *et al.*, 2002; Desikan *et al.*, 2006). The resulting cerebellum region of interest (grey matter only) was used as a reference region to create a PiB DVR image. The resulting brainstem region of interest by the FreeSurfer processing stream was manually edited to generate a pons region of interest that was used to normalize FDG data for each individual. Large cortical regions of interest spanning frontal, temporal, and parietal cortices, and anterior/posterior cingulate gyri were constructed as previously described (Oh *et al.*, 2011). Mean DVR values from these large regions of interest constituted a global PiB index for each subject.

To account for voxelwise grey matter volume differences in the whole-brain voxelwise analyses of the FDG data across

groups, we performed voxel-based morphometry (VBM) implemented with SPM8 running under Matlab 7.7 (Mathworks, Natick, MA) on structural images. VBM is a semi-automated iterative procedure in which implementations of tissue classification, bias correction, and non-linear warping are combined. Details can be found in a previously published report (Oh *et al.*, 2011). Voxelwise grey matter volume images as a covariate consisted of unmodulated warped images that were smoothed with a 12-mm Gaussian kernel at the full-width and half-maximum.

Although our main analyses were performed on PET data uncorrected for partial volume effect, we performed partial volume correction (PVC) on PiB and FDG data using a two-compartment model (Meltzer *et al.*, 1999). PVC-PET data results are provided in the [Supplementary material](#).

Region of interest analyses of Pittsburgh compound B and fluorodeoxyglucose data

To determine relationships between amyloid- β deposition and high and low glucose metabolism in young adults, we extracted FDG counts and PiB DVRs, for each subject, from 20 FreeSurfer-defined cortical regions of interest from each hemisphere that comprise most of the cortical regions except for primary motor and somatosensory cortices and visual cortex. In addition, three subcortical regions (i.e. caudate, putamen, and hippocampus) from each hemisphere were included in the analysis. We took a conservative approach by particularly focusing on these *a priori* regions of interest rather than including all FreeSurfer-based regions of interest based on the known distribution of amyloid- β deposition (e.g. primary sensory and motor cortices do not exhibit amyloid- β deposition) and their functional relevance to Alzheimer's disease (e.g. hippocampus). FDG and PiB data were extracted from a total of 46 brain regions, and due to significant signal loss in the frontal pole regions of interest, 44 regions of interest were included for further analysis. Among 44 regions of interest, 11 cortical regions of interest that fell in the top quartile of regions of interest in terms of FDG values were identified as the highest glucose metabolism regions in young adults, while another 11 cortical regions of interest that consisted of the bottom quartile of regions of interest were classified as the lowest glucose metabolism regions in young adults. FDG and PiB values were volume and age adjusted within each group and averaged across 11 regions of interest in each high and low glucose metabolism region.

Whole-brain voxelwise analyses of fluorodeoxyglucose data

Pons-normalized FDG images warped to an MNI structural template were used for whole-brain voxelwise analyses. Comparisons of whole-brain voxelwise FDG data across groups were conducted using the Robust Biological Parametric Mapping (rBPM) toolbox, treating subjects as a random factor. Robust Biological Parametric Mapping allows for the inclusion of voxelwise regressors and implements a robust regression model (using the bisquare weight function) to reduce sensitivity to outliers. For the comparison of young

and PiB- OLD groups, analysis of covariance (ANCOVA) was applied to voxelwise FDG data with sex, apolipoprotein $\epsilon 4$ (*APOE4*) and VBM-processed grey matter volume maps being included as nuisance regressors. The association between amyloid- β deposition and glucose metabolism among cognitively normal older adults was assessed by treating PiB index as a continuous independent variable with age, sex, *APOE4* carrier status, and grey matter volume maps as nuisance regressors. For the comparison of PiB+ OLD and Alzheimer's disease groups, ANCOVA was applied to voxelwise FDG data with age, sex, *APOE4* carrier status, and grey matter volume maps as nuisance regressors. Significant clusters were determined at least at $P < 0.05$ at voxel level and $P < 0.05$ at cluster level (a cluster size > 640 voxels). Suprathreshold clusters were projected on to semi-inflated brain surfaces using Caret v5.64 software.

Statistical analyses

All non-image analyses were conducted using SPSS software (version 21). Two-sample *t*-tests were used to assess the difference in averaged FDG and PiB values between the highest and lowest glucose metabolism regions as defined by young adults within each group. One-way analysis of variance (ANOVA) was conducted to evaluate group differences in FDG values and two-way ANOVAs were conducted for testing group by region interactions. *Post hoc* tests were followed and statistical significance was determined using false discovery rate (Benjamini and Hochberg, 1995) correction for multiple comparisons. Multiple regressions were used to assess the relationship between global PiB index and regional FDG values with age, sex, *APOE4* carrier status, and region of interest volume being controlled. Statistical significance for all tests was determined at $P < 0.05$, two-tailed.

Results

Regional differences in glucose metabolism across young, older cognitively normal, and Alzheimer's disease groups

As previously described (Oh *et al.*, 2011), all three neuroimaging datasets were coregistered to a PiB-PET image in native space for each subject, and using an averaged single structural T_1 image processed through FreeSurfer v4.4, we implemented region of interest labelling and extracted FDG and PiB values from *a priori* selected 20 cortical regions of interest and three subcortical regions in native space from each hemisphere. The FDG and PiB values for each region of interest are plotted by group in each hemisphere (Fig. 1 and [Supplementary Fig. 1](#)). The highest glucose metabolism regions in youths were defined as the top quartile of the cortical regions of interest in young subjects. These regions included rostral and caudal middle frontal gyri bilaterally, right precuneus, inferior parietal cortex bilaterally, inferior frontal gyrus pars opercularis bilaterally, and inferior frontal gyrus pars triangularis bilaterally. The lowest regional

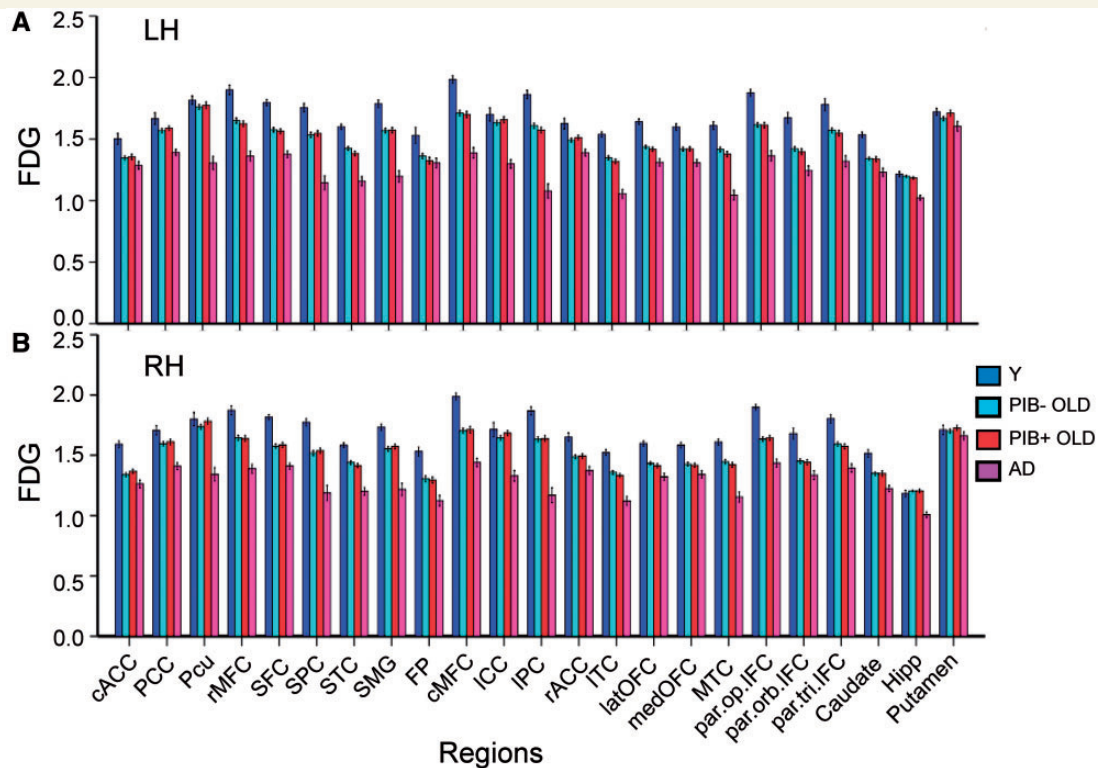


Figure 1 Regional variation of FDG by group. FDG values normalized to each subject's pons (FDG SUVR) are plotted by group for each region of interest in left (A) and right (B) hemispheres. Data are presented as mean \pm SD. cACC = caudal anterior cingulate cortex; cMFC = caudal middle frontal cortex; FP = frontal pole; Hipp = hippocampus; ICC = isthmus cingulate cortex; IPC = inferior parietal cortex; ITC = inferior temporal cortex; latOFC = lateral orbitofrontal cortex; LH = left hemisphere; medOFC = medial orbitofrontal cortex; MTC = middle temporal cortex; par.op.IFC = inferior frontal cortex pars opercularis; par.orb.IFC = inferior frontal cortex pars orbitalis; par.tri.IFC = inferior frontal cortex pars triangularis; PCC = posterior cingulate cortex; Pcu = precuneus; rACC = rostral anterior cingulate cortex; RH = right hemisphere; rMFC = rostral middle frontal cortex; SFC = superior frontal cortex; SMG = supramarginal gyrus; SPC = superior parietal cortex; STC = superior temporal cortex; Y = young.

glucose metabolism in young subjects, the bottom quartile of cortical regions of interest, was in caudal anterior cingulate cortex bilaterally, superior, middle, and inferior temporal cortices bilaterally, lateral orbital frontal cortex bilaterally, and right medial orbital frontal cortex. The PiB counts extracted for each region of interest were used to compute PiB values for larger cortical regions of interest in subsequent analyses. The results from PVC-PET data are provided in [Supplementary Figs 2 and 3](#). Except for frontal pole, the overall results remained similar to non-PVC data.

Relationship between glucose metabolism in young adults and amyloid- β deposition

To quantify the relationship between the degree of glucose metabolism measured in young adults and amyloid- β deposition during ageing, mean FDG and PiB values from the highest and lowest glucose metabolism regions of interest (defined in young subjects) were averaged separately within

the high and low regions for each group. We found significantly higher glucose metabolism in the highest compared to the lowest glucose metabolism regions in young ($T = 12.85$, $P < 0.001$), PiB- OLD ($T = 6.66$, $P < 0.001$) and PiB+ OLD ($T = 10.62$, $P < 0.001$) groups while the regional difference disappeared in Alzheimer's disease patients ($T = 1.00$, $P > 0.05$) ([Fig. 2A](#)). With PiB data, however, we found significantly higher PiB retention in the highest compared to the lowest glucose metabolism regions within the PiB+ group ($T = 2.05$, $P < 0.05$), while other groups did not show a significant difference between the two regions (young subjects: $T = 1.1$, $P = 0.3$; PiB- OLD: $T = 1.4$, $P = 0.2$; Alzheimer's disease: $T = 1.0$, $P = 0.3$) ([Fig. 2B](#)). This regional difference in PiB retention between the highest and lowest glucose metabolism regions was confirmed by a correlation analysis showing a significant positive relationship between the region of interest FDG values from young subjects and the region of interest PiB values from the PiB+ group when all regions of interest were included ($R = 0.3$, $P = 0.05$) ([Supplementary Fig. 4](#) for both non-PVC and PVC data results).

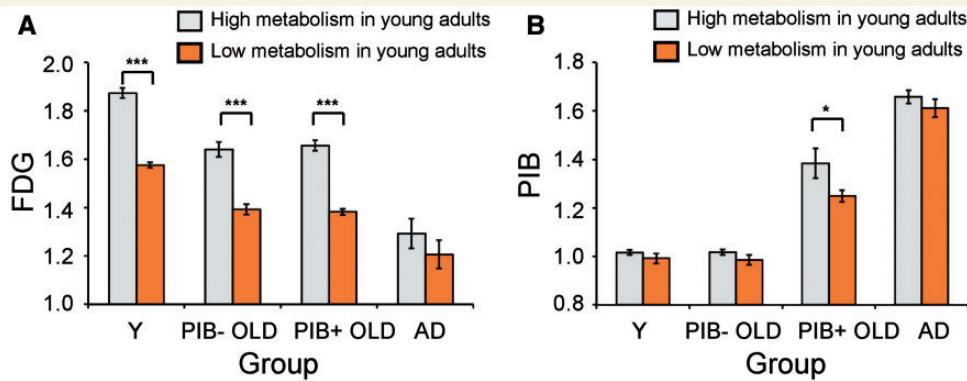


Figure 2 Brain regions accumulating greater amyloid- β show higher glucose metabolism in young adults compared to other regions. Mean FDG SUVR (A) and PiB DVR (B) values from high (grey bars) and low (orange bars) glucose regions defined in young adults are plotted by group. For FDG, significant differences between high and low baseline glucose regions were shown in young, PiB- OLD, and PiB+ OLD (P -values < 0.001). For PiB, a significant difference was only observed in PiB+ OLD group ($P < 0.05$). Data are presented as mean \pm standard error of the mean (SEM). * $P < 0.05$; *** $P < 0.001$.

Whole-brain voxelwise mean distribution of FDG and PiB across groups

To confirm region of interest-based classification of high and low glucose metabolism regions in young adults and visualize the specific spatial correspondence between high glucose metabolism in young adults and high amyloid- β deposition in PiB+ cognitively normal older adults, we examined the whole-brain voxelwise mean distribution of FDG and PiB data overlaid on brain surfaces for each group (Fig. 3). The spatial distribution of glucose metabolism in young subjects (Fig. 3A) was well matched with the region of interest-based classification of the highest and lowest glucose metabolism regions (Fig. 3E). Topography of PiB binding only in the PiB+ OLD group (Fig. 3G) overlapped with the spatial distribution of higher glucose metabolism in young subjects (Fig. 3A). Patients with Alzheimer's disease showed low glucose metabolism (Fig. 3D) and high PiB binding across the whole brain with little regional differentiation (Fig. 3H).

Regional differences in age and amyloid- β -dependent changes in glucose metabolism

Although our primary interest was to assess age and amyloid- β -related changes in glucose metabolism, we examined a group effect in regional amyloid deposition along with glucose metabolism by applying omnibus one-way ANOVAs (group as a factor) to PiB and FDG data for each region of interest, followed by *post hoc* tests (false discovery rate correction for multiple comparisons). With PiB data, we predictably found a significant group effect in most regions of interest with a similar pattern of changes across groups: no difference between young and

PiB- OLD groups but significant increases in PiB values in PiB+ OLD and Alzheimer's disease patients groups compared to PiB- OLD and PiB+ OLD groups, respectively (P -values < 0.05 ; Fig. 4, and Supplementary Figs 5 and 6). In hippocampus, PiB values were significantly higher in only PiB+ OLD subjects compared to the other groups ($P < 0.05$; Supplementary Fig. 6). Omnibus one-way ANOVAs with FDG data showed a significant group effect in all regions of interest except for the left and right putamen (P -values < 0.05), but *post hoc* tests revealed regional differences in the pattern of age and amyloid- β -related changes in glucose metabolism. Regions of interest that show a similar pattern of age and amyloid- β -related changes in glucose metabolism were combined within each cortical lobe for subsequent analyses to minimize the number of comparisons. The regions of interest of frontal, temporal, and lateral parietal cortex, and the caudate nucleus showed a significant age-related reduction in glucose metabolism but no amyloid- β -related changes (but see the whole-brain voxelwise results below), along with a significant reduction in glucose metabolism due to Alzheimer's disease symptoms (Fig. 4A and Supplementary Fig. 5). For precuneus, posterior cingulate cortex and two subcortical regions (putamen and hippocampus), however, there was no significant age or amyloid- β -related difference in glucose metabolism, while, except for putamen, these brain regions showed Alzheimer's disease-related reduction in glucose metabolism (Fig. 4B and Supplementary Fig. 6). Two-way ANOVAs with region (e.g. frontal cortex and precuneus) and group as factors (Fig. 4C) further confirmed the different pattern of glucose metabolism changes due to age and amyloid- β deposition between precuneus and frontal cortex (right hemisphere: $F = 7.69$, $P < 0.001$; left hemisphere: $F = 8.69$, $P < 0.001$). Besides these patterns of changes in glucose metabolism, only age-related reduction in glucose metabolism with no significant effects of amyloid- β and

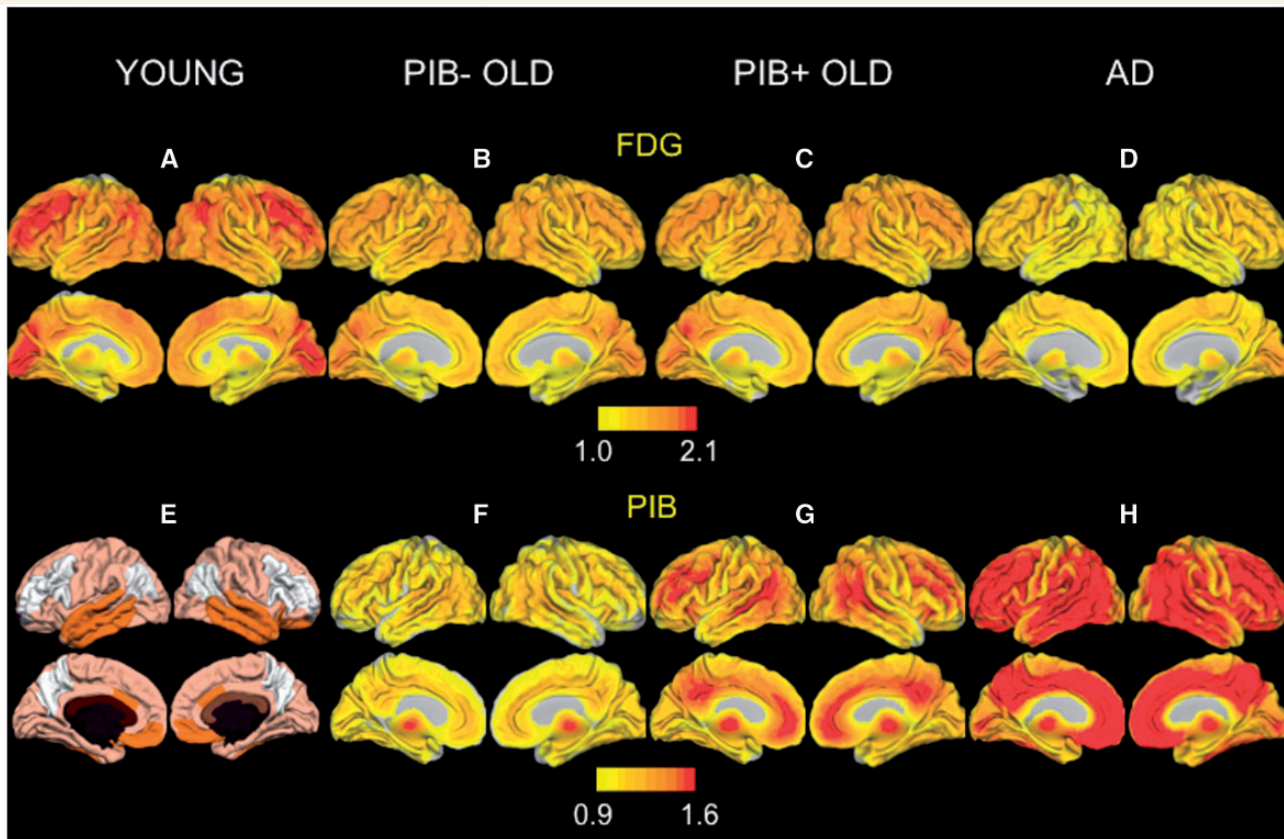


Figure 3 Voxel-wise mean glucose metabolism and PiB binding across young, PiB- OLD, PiB+ OLD, and Alzheimer's disease subjects. Voxel-wise mean FDG and PiB values are overlaid on semi-inflated lateral and medial surfaces of the brain for young (A), PiB- OLD (B and F), PiB+ OLD (C and G), and Alzheimer's disease (D and H) groups. The top row (A–D) displays the FDG data while the bottom row (F–H) displays the PiB data with an exception that, for young subjects (E), a map of region of interest-based high (grey) and low (orange) metabolism regions is shown instead of the PiB data. Scale represents raw FDG SUVR and PiB DVR values, respectively.

Alzheimer's disease was observed in the left anterior cingulate cortex ($F = 5.07$, $P = 0.002$).

Although not significant at a group level, a trend of metabolic increases with amyloid- β deposition between PiB- and PiB+ OLD groups was observed in the right precuneus. Using the global PiB index as a continuous variable, we tested an association between global PiB index and FDG in the right precuneus among cognitively normal older adults and found a significant positive association between global PiB index and regional FDG in right precuneus, accounting for age, sex, *APOE4* status, and region of interest volume, $\beta = 0.3$, $P < 0.05$ (Fig. 5). The regional FDG in right precuneus was also significantly associated with *APOE4* carrier status, showing significant reduction in FDG in right precuneus with *APOE4* carriers ($\beta = -0.21$, $P < 0.05$). We examined an association between global PiB index and glucose metabolism in other regions typically showing Alzheimer's disease-related hypometabolism, including left precuneus, lateral inferior parietal cortex, and posterior cingulate regions. Although similar positive trends were observed, no region showed significant hypermetabolism in relation to amyloid- β deposition (Supplementary Table 1).

To confirm region of interest results of age and amyloid- β -related changes in regional glucose metabolism and to examine any regions that region of interest-based analyses might have missed, we conducted exploratory whole-brain voxelwise analyses. A voxelwise comparison of FDG data between young and PiB- OLD groups with sex, *APOE4* status, voxelwise grey matter volume as covariates revealed significant age-related reduction in most brain regions, but also showed the age-invariant preservation of FDG in voxels within precuneus, posterior cingulate, lateral middle and inferior frontal and temporoparietal cortices, hippocampus, and primary sensorimotor cortex (Fig. 6A). For amyloid- β -related changes in glucose metabolism, we regressed the voxelwise FDG data on a global PiB index as a continuous variable with PiB- and PiB+ groups combined. Age, sex, *APOE4* status, and voxelwise grey matter volume were controlled in this analysis. Supporting the region of interest results, brain regions including posterior cingulate and precuneus showed amyloid- β -related hypermetabolism, which was additionally found in anterior cingulate cortex, medial frontal cortex, and lateral middle and superior frontal cortices (Fig. 6B).

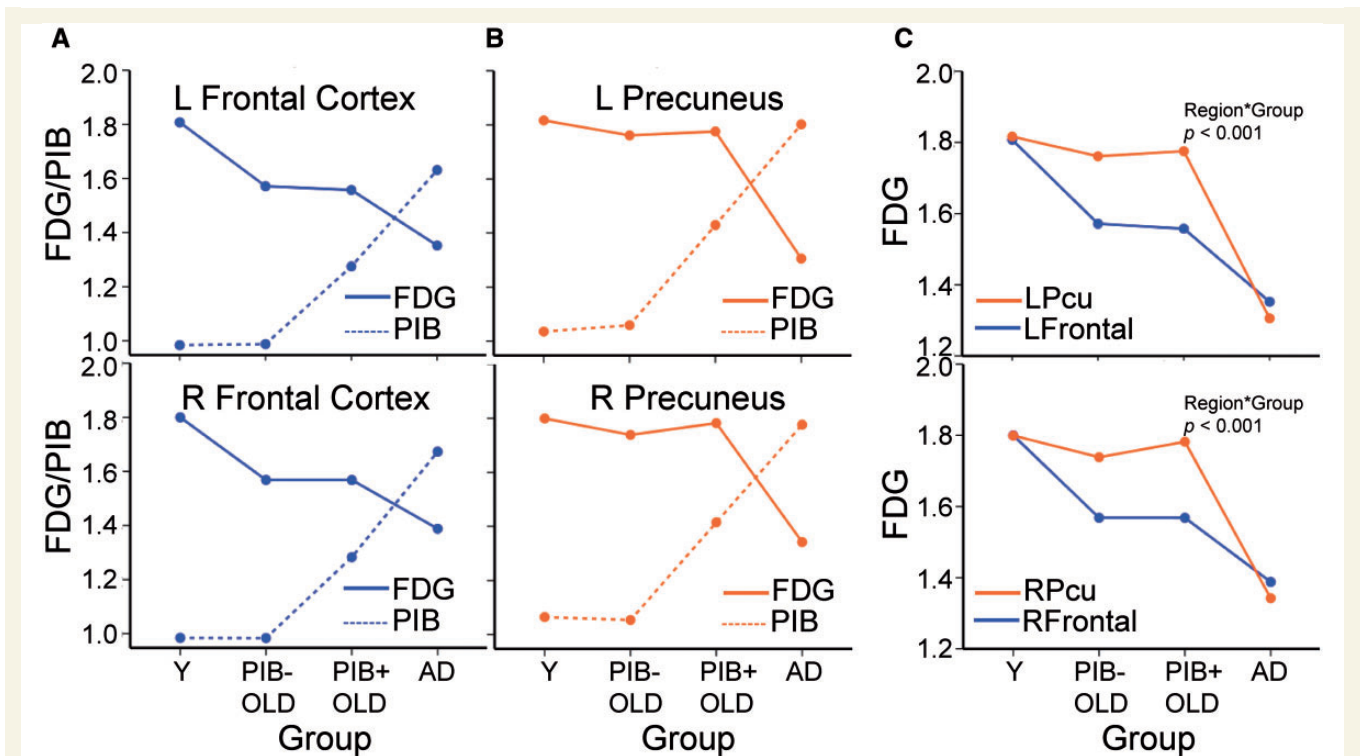


Figure 4 Regional variation in age, amyloid- β , and Alzheimer's disease-related changes in glucose metabolism. Regional FDG SUVR (solid lines) and PiB DVR (dotted lines) values are plotted for frontal cortex (A) and precuneus by hemisphere (B). FDG SUVR values from frontal cortex (Frontal) and precuneus (Pcu) are plotted to demonstrate a significant interaction effect between region and group (C). Similar patterns of FDG and PiB across groups were observed in frontal, parietal and temporal cortices, and caudate. Posterior cingulate cortex, putamen, and hippocampus regions of interest showed a pattern of FDG change across groups that resembles precuneus. L = left; R = right; Y = young.

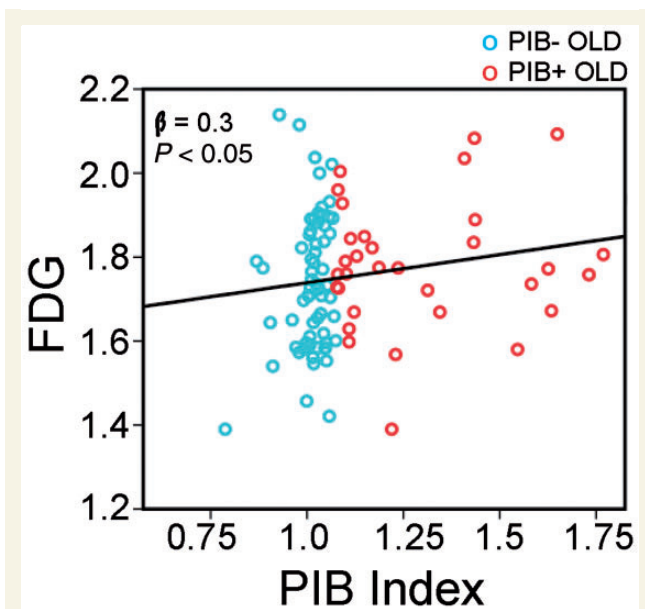


Figure 5 Relationships between right precuneus FDG and global PiB index in cognitively normal older adults. Right precuneus FDG was positively correlated with global PiB index, controlling for age, sex, *APOE4* carrier status, and region of interest volume among cognitively normal older adults.

No region showed amyloid- β -related hypometabolism. By comparing PiB+ OLD and Alzheimer's disease subject groups with age, sex, *APOE4* carrier status, and voxelwise grey matter volume controlled, Alzheimer's disease-related hypometabolism was found in lateral temporoparietal cortex, posterior cingulate/precuneus, lateral middle frontal cortex, and hippocampus (Fig. 6C). PVC data showed the similar results with even stronger trend to the same direction (Supplementary Fig. 7).

Discussion

We examined a possible mechanism underlying the regional vulnerability to amyloid- β deposition and Alzheimer's disease-related hypometabolism. Consistent with previous studies, regional variations existed in glucose metabolism across brain regions in all groups. A novel finding is that the differences in glucose metabolism between regions with the highest and lowest glucose metabolism defined in young subjects persist across the lifespan, even in those who accumulate amyloid- β . However, in those who deposit amyloid- β , PiB binding was greater in brain regions with the highest metabolism in young subjects, direct evidence in support of a link between early life glucose metabolism

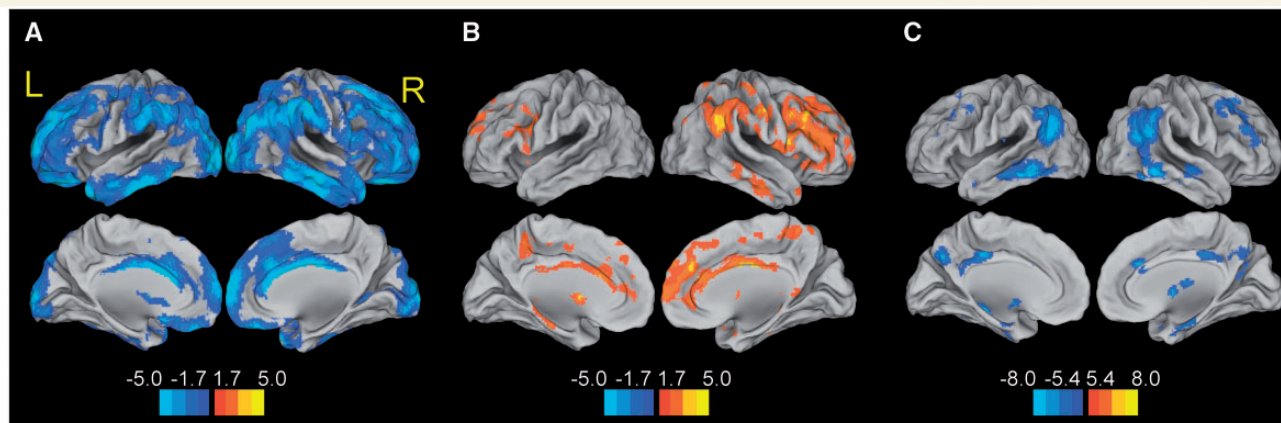


Figure 6 Exploratory whole-brain voxelwise analyses of age, amyloid- β , and Alzheimer's disease-related changes in glucose metabolism. A whole-brain voxelwise comparison between young and PiB- OLD group revealed brain regions showing lower FDG (cool colours) in PiB- OLD compared to young subjects (**A**) and a multiple regression model with PiB index as a continuous variable shows increased FDG in some brain regions (warm colours) with higher PiB index (**B**). A whole-brain voxelwise comparison between PiB+ OLD and Alzheimer's disease groups shows characteristic Alzheimer's disease-related hypometabolism (**C**). Gender, *APOE4* status, and voxelwise grey matter volume was controlled in all analyses, and age was additionally controlled in **B** and **C**. Significant clusters were determined at $P < 0.05$ at voxel level and $P < 0.05$ at cluster level (a cluster size > 640 voxels) for **A** and **B**. A higher threshold at voxel level (FWE, $P < 0.05$) was applied to **C**. Scales represent *T*-values. L = left hemisphere; R = right hemisphere.

and amyloid- β deposition. While age-related reduction was uniformly observed across most brain regions, we also found brain regions showing age-invariance in glucose utilization. These regions include the precuneus, posterior cingulate cortex, lateral middle frontal and temporoparietal cortex, putamen, and hippocampus. In addition, cognitively intact older adults with higher levels of amyloid- β deposition showed stable or increased glucose metabolism in some of these brain regions, particularly in lateral frontoparietal cortices, precuneus and hippocampus. While amyloid- β deposition is found throughout the brain, brain regions conjunctively exhibiting age-invariant glucose metabolism and amyloid- β -related hyper-metabolism were most susceptible to Alzheimer's disease-related hypometabolism.

Relationships between glucose metabolism in young adults and amyloid- β deposition

There is great interest in understanding the causal factors underlying amyloid- β deposition. Consistent with findings from animal studies (Bero *et al.*, 2011) showing relationships between neural activity and amyloid- β plaque formation in cingulate and piriform (analogous to precuneus in humans) cortex, Alzheimer's disease patients commonly show increased amyloid- β deposition in brain regions comprising the DMN (Raichle *et al.*, 2001; Buckner *et al.*, 2009), possibly reflecting greater metabolic demands prior to amyloid- β accumulation. Consistent with findings in the animal studies and propositions based on human research,

we found overlapping topography of greater glucose metabolism in young people and increased amyloid- β deposition in older people in a set of brain regions including precuneus and lateral parietal cortex that have been considered as part of the DMN.

Several recent human neuroimaging studies provide ample evidence supporting a possible link between regional increases of metabolic demand and network-level functional properties of the brain. Some evidence comes from studies that have found that brain regions defined as cortical hubs, such as posterior cingulate cortex/precuneus, lateral parietal and temporal cortices, express disproportionately more connections with other brain regions and a map of such hubs shows a high correspondence with amyloid- β deposition in patients with Alzheimer's disease (Buckner *et al.*, 2009). Moreover, these studies have shown that cortical hubs were associated with multiple but functionally distinct networks including the frontoparietal control network (FPCN) and DMN, suggesting the hubs' involvement in multiple functional networks. This is consistent with the recent findings that the subdivisions of posterior cingulate cortex were differentially connected with other brain regions both functionally and anatomically (Buckner *et al.*, 2008; Leech *et al.*, 2011) and precuneus was associated with both DMN and FPCN (Vincent *et al.*, 2008). As more evidence, the FPCN, which strongly overlaps with high glucose metabolism regions in young subjects in the present study, is a brain network constantly switching between the DMN and dorsal attention network (DAN) (Vincent *et al.*, 2008; Spreng and Schacter, 2012). Furthermore, not only is the engagement in multiple functional networks related to metabolic activity but so is

connectivity distance: functional connectivity of long-distance connections is more strongly correlated with metabolism than that of short-distance connections (Liang *et al.*, 2013). Not surprisingly, the topography of high glucose metabolism in young adults in the present study shows a high convergence with brain regions expressing long-distance connections and strong functional connectivity (Liang *et al.*, 2013). In a recent study, amyloid- β -related alterations in functional connectivity were found to be more pronounced in brain regions involved in multiple networks among cognitively normal elderly (Elman *et al.*, 2016). Therefore, guided by the general principle of the relationships between synaptic activity, metabolic demand, and amyloid- β deposition, it is possible that brain regions implicated in several functional networks may be more active both neurally and metabolically, resulting in higher amyloid- β deposition during ageing. To our knowledge, the present study is the first showing a direct relationship between glucose metabolism in young adults and amyloid- β deposition in humans.

Interestingly, however, discordance between the topography of glucose metabolism in young adults and amyloid- β deposition was observed in some brain regions: low glucose metabolism in young adults but high amyloid- β deposition was seen in medial frontal cortex, anterior cingulate cortex, and lateral temporal cortex while high young adulthood glucose metabolism but low amyloid- β deposition was seen in visual cortex. Although the exact nature of these discordant relationships is not clear, these observations together may relate to several accounts of functional organization of the brain, some of which have been discussed above. For instance, the visual cortex, which showed high metabolism in young adults but low amyloid- β deposition, is a brain region whose functional connectivity is primarily short-distance (Liang *et al.*, 2013). Although speculative, this interpretation is in line with the idea that amyloid spreads through long-range connections in the brain rather than proximity-wise progression (Pearson and Powell, 1989).

Discordance between low glucose metabolism in young adults and high amyloid- β deposition is difficult to interpret, because it is not parsimoniously explained by the life-long metabolism-dependent cascade hypothesis and may suggest an additional mechanism involved. Considering an independent pathway of pathogenesis of the medial temporal lobe-mediated tauopathy and recent findings that showed a strong correlation between amyloid- β plaques in the medial temporal lobes (hippocampus and parahippocampus) and increased amyloid- β deposition in orbitofrontal, and lateral temporal cortex in patients with Alzheimer's disease (Sepulcre *et al.*, 2013), it is possible that amyloid- β deposition in brain regions of older adults, defined by low glucose metabolism in young adults, may be due to a separate medial temporal lobe-mediated tau pathology. In this scenario, tau deposition, perhaps via aberrant neural activity, results in amyloid- β deposition in efferent target regions including medial PFC and lateral temporal lobes, regions

with well-known connectivity to the medial temporal lobe (Ranganath and Ritchey, 2012). This interpretation is consistent with previous findings that efferent target regions such as medial frontal cortex and posterior cingulate cortex/precuneus are affected by Alzheimer's disease-related pathological changes (i.e. neurofibrillary tangles and amyloid- β) in medial temporal lobe (Pearson and Powell, 1989; Khan *et al.*, 2014). An alternative hypothesis, however, would be that these regions develop amyloidosis secondarily, because of incipient amyloidosis in brain regions with higher metabolism. This model seems to fit the present data as well because the difference in amyloid between regions with low- and high-metabolism is not seen in patients with Alzheimer's disease. With the advent of tau PET, future research investigating these possible mechanisms is promising.

Regional differences in age and amyloid- β -related changes in glucose metabolism

Even though the topography of amyloid- β deposition is widespread across the brain during the progression of Alzheimer's disease, Alzheimer's disease-related hypometabolism is more severe in posterior brain regions involving the posterior part of the DMN (Minoshima *et al.*, 1997; Klunk *et al.*, 2004; Buckner *et al.*, 2005; Edison *et al.*, 2007; Landau *et al.*, 2011). Because several neuronal insults involving tauopathy, brain atrophy, and synaptic loss might have already started before the clinical diagnosis of Alzheimer's disease, it is unclear to what extent amyloid- β deposition contributes to metabolic changes during the progression of Alzheimer's disease, particularly in the early stage of Alzheimer's disease pathology. Furthermore, not only Alzheimer's disease-related pathological biomarkers but also ageing itself has been shown to contribute to metabolic changes. Consistent with previous studies, we found age-related hypometabolism in most brain regions but preserved glucose metabolism in some brain regions such as posterior cingulate, precuneus, hippocampus, and part of lateral frontal and temporoparietal cortices during ageing, which was more evident in a voxelwise analysis (Kalpouzos *et al.*, 2009). A mechanistic view linking age-invariance in glucose metabolism to the progression to Alzheimer's disease-related hypometabolism, however, has been lacking so far. Although preserved metabolism with ageing might seem a beneficial process that could maintain normal cognition, the data suggesting that higher metabolism could lead to amyloid- β deposition raises the possibility that this continued metabolic demand throughout lifetime may predispose these regions to be more vulnerable to neural insult in the long run. The topography of brain regions showing age-invariant glucose metabolism further parallels brain regions following the ontogenetic and phylogenetic model (i.e. the 'last-in first-out' rule) in brain development and ageing, suggesting that the brain regions exhibiting

steeper brain atrophy during ageing may be the regions showing constant metabolic demand throughout the lifetime (Douaud *et al.*, 2014), although those might not be the regions showing the highest metabolism in young adults. Another possible explanation is that brain regions, such as lateral frontal cortex, that undergo age-related hypometabolism, might have been already affected in cognitively normal older adults so that not much difference is detected when compared to Alzheimer's disease patients, while brain regions showing age-invariant glucose metabolism may be differentiated in this regard as illustrated by a significant interaction effect between brain regions and group (i.e. the data presented in Fig. 4). It is important to note that subregions within the lateral frontal and parietal cortices showed preserved glucose metabolism, which was more evident in voxelwise analyses, while not being detected in region of interest-based analyses, suggesting functional heterogeneity within these large structures. These two possibilities, however, are not mutually exclusive, but rather contribute together to the differential regional vulnerability to Alzheimer's disease-related hypometabolism.

With regard to the relationship between amyloid- β deposition and glucose metabolism during ageing, several animal studies using APP transgenic mouse models have shown amyloid- β -related hyperactivity of neurons, which becomes exacerbated with the presence of tau (Busche *et al.*, 2008; Palop and Mucke, 2010; Roberson *et al.*, 2011). Therefore, it is not surprising to find an overlapping topography between amyloid- β deposition and hypermetabolism in cognitively normal older adults with amyloid burden, which additionally fits well with the animal literature showing an inverted U relationship between amyloid deposition and heightened neuronal activity (Palop and Mucke, 2010). In addition, amyloid- β deposition not only results in heightened excitability of neurons but also produces microgliosis, astrocytosis, and the overproduction and release of various inflammatory mediators that may explain the increased glucose metabolism (Fellin *et al.*, 2004; Vezzani and Granata, 2005; Palop and Mucke, 2010). This seemingly robust relationship between amyloid- β deposition and hypermetabolism, however, remained controversial in human studies, in part due to different methodologies and inconsistent results across studies. Previous studies reporting hypermetabolism in relation to amyloid- β deposition used multivariate methods using covariance analysis (Oh *et al.*, 2014) or modelling based on estimated years from expected symptom onset (Bateman *et al.*, 2012; Benzinger *et al.*, 2013). Studies using a univariate approach found a trend level of significance with regional PiB counts (Ossenkoppele *et al.*, 2014). Moreover, some studies reported the opposite findings of amyloid- β -related hypometabolism during ageing (Lowe *et al.*, 2014), although Alzheimer's disease-invariant FDG in putamen, one of the *a priori* regions in our study, confirms that our findings are consistent with those of other studies (Shin *et al.*, 2011). While more systematic investigation

will be necessary to resolve these opposite results, it is possible that these seemingly incompatible findings may suggest a non-linear relationship between glucose metabolism and amyloid- β deposition during the progression of Alzheimer's disease pathology, which will require longitudinal studies.

Although our results show that brain regions undergoing amyloid- β -related increases but age-related invariance in glucose metabolism are more prone to hypometabolism in Alzheimer's disease, some regions clearly deviate from this prediction. Amyloid- β -related hypermetabolism in cognitively normal older adults was also found in anterior cingulate cortex and medial frontal cortex, but these regions do not exhibit evident hypometabolism during Alzheimer's disease. Further, the lateral temporal cortex exhibits clear hypometabolism in Alzheimer's disease but not amyloid- β -related hypermetabolism (more so in the left hemisphere) in cognitively normal older adults. The former regions do not exhibit age-invariance in glucose metabolism, while the latter regions do. Therefore, while the brain regions jointly affected by both amyloid- β -related hypermetabolism and age-invariant metabolism are the most vulnerable regions that undergo hypometabolism with the disease state of Alzheimer's disease, other regions also show a graded level of hypometabolism depending on how strongly the regions exhibit the life-long characteristics of glucose utilization. An alternative, but related, possibility is that the regions exhibiting the conjoint features of age and amyloid- β -related metabolic changes such as posterior cingulate/pre-cuneus and hippocampus may be core regions that lead to increased hypometabolism in other regions in the disease state of Alzheimer's disease. Because the lateral temporoparietal cortices, for example, are anatomically and functionally connected with these core regions, the regions showing discrepancy may be subsequently affected through these connections as postulated in previous studies (Lehmann *et al.*, 2013).

Based on the present cross-sectional study, however, the causality between glucose metabolism and amyloid- β deposition among cognitively normal older adults with amyloid- β , cannot be determined. That is, increased glucose metabolism can be a response to higher level of amyloid- β accumulation (Busche *et al.*, 2008; Palop and Mucke, 2010), while concurrent amyloid- β -induced hyperactivity can lead to a vicious cycle of increased production and release of amyloid- β . Although the present study cannot disentangle these two alternative explanations for amyloid- β -related hypermetabolism, our results suggest that regionally varying associations between age, amyloid- β deposition, and glucose metabolism together account for the regional vulnerability to Alzheimer's disease-related hypometabolism.

Limitations of the study

Several limitations of our study need to be mentioned. Although glucose metabolism in young adults was

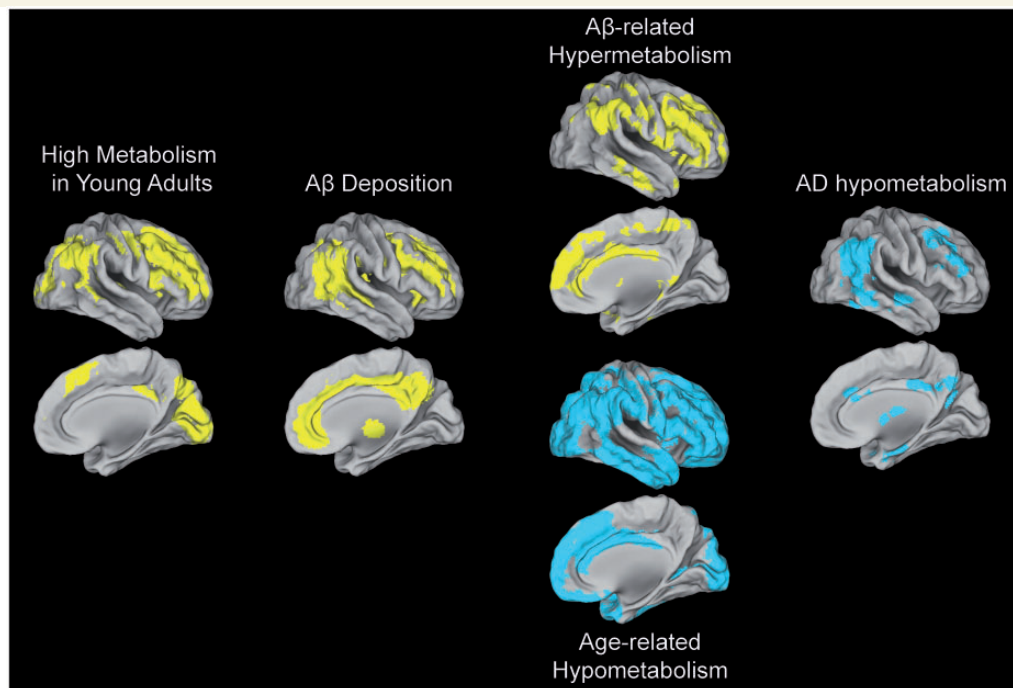


Figure 7 Hypothetical relationships between baseline glucose metabolism, amyloid- β deposition, age and amyloid- β -related metabolic changes, and Alzheimer's disease hypometabolism. A β = amyloid- β .

significantly associated with amyloid- β deposition in PiB+ older adults, incomplete concordance between the two measures was also observed in brain regions such as medial frontal, lateral temporal, and anterior cingulate cortices. Although we speculate that amyloid- β deposition in these brain regions may be accounted for by a different mechanism (e.g. medial temporal lobe-mediated pathology or secondary amyloidosis) other than the life-long metabolism-dependent cascade, this remains hypothetical. In addition, we cannot draw a causal directionality between FDG changes (i.e. hypermetabolism) and amyloid- β accumulation in older PiB+ subjects. Although modelling studies based on cross-sectional data have suggested a longitudinal trajectory of temporarily increased glucose metabolism with amyloid- β deposition (Benzinger *et al.*, 2013), longitudinal studies examining the directionality between glucose metabolism and amyloid- β deposition will be needed to clearly delineate the causal relationship between these biomarkers during ageing. Another limitation that needs to be mentioned is a small sample size of young individuals included in the present study. Future studies with a larger sample representing young adults will be necessary to detect the age-related effect in a more robust manner and to account for any sample-related variance.

Conclusion

In the present study, we tested whether regionally specific vulnerability to amyloid- β deposition and hypometabolism

during the progression of Alzheimer's disease relates to regional differences in glucose metabolism in young adulthood and age and amyloid- β -related metabolic changes during ageing. As summarized in Fig. 7, we found that higher glucose metabolism in youths is related to regionally-specific increases in amyloid- β accumulation. Not all brain regions deposited with amyloid- β , however, did undergo Alzheimer's disease-related hypometabolism. Among those, brain regions expressing an age-invariant metabolic demand and amyloid- β -related hypermetabolism undergo greater hypometabolism during clinical Alzheimer's disease. It is worth noting that incomplete concordance between glucose metabolism in young adults and amyloid- β deposition was observed in some brain regions, and we speculate that a tau-mediated mechanism or secondary amyloidosis may play a role in later amyloid- β deposition and Alzheimer's disease-related neurodegeneration in these discordant regions. In conclusion, the present findings provide evidence suggesting a mechanism underlying differential regional vulnerability to amyloid- β deposition and Alzheimer's disease-related hypometabolism via constant metabolic demands across the lifespan as well as in the presence of amyloid- β pathology.

Funding

This study was supported by the Alzheimer's Association and National Institute on Aging grant (R01-AG034570) to W.J.J.

Supplementary material

Supplementary material is available at *Brain* online.

References

- Bateman RJ, Xiong C, Benzinger TL, Fagan AM, Goate A, Fox NC, et al. Clinical and biomarker changes in dominantly inherited Alzheimer's disease. *N Engl J Med* 2012; 367: 795–804.
- Benjamini Y, Hochberg Y. Controlling the false discovery rate: a practical and powerful approach to multiple testing. *J R Stat Soc B (Methodol)* 1995; 57: 289–300.
- Bennett DA, Schneider JA, Arvanitakis Z, Kelly JF, Aggarwal NT, Shah RC, et al. Neuropathology of older persons without cognitive impairment from two community-based studies. *Neurology* 2006; 66: 1837–44.
- Benzinger TL, Blazey T, Jack CR, Jr, Koeppe RA, Su Y, Xiong C, et al. Regional variability of imaging biomarkers in autosomal dominant Alzheimer's disease. *Proc Natl Acad Sci USA* 2013; 110: E4502–9.
- Bero AW, Yan P, Roh JH, Cirrito JR, Stewart FR, Raichle ME, et al. Neuronal activity regulates the regional vulnerability to amyloid-beta deposition. *Nat Neurosci* 2011; 14: 750–6.
- Buckner RL, Andrews-Hanna JR, Schacter DL. The brain's default network: anatomy, function, and relevance to disease. *Ann N Y Acad Sci* 2008; 1124: 1–38.
- Buckner RL, Sepulcre J, Talukdar T, Krienen FM, Liu H, Hedden T, et al. Cortical hubs revealed by intrinsic functional connectivity: mapping, assessment of stability, and relation to Alzheimer's disease. *J Neurosci* 2009; 29: 1860–73.
- Buckner RL, Snyder AZ, Shannon BJ, LaRossa G, Sachs R, Fotenos AF, et al. Molecular, structural, and functional characterization of Alzheimer's disease: evidence for a relationship between default activity, amyloid, and memory. *J Neurosci* 2005; 25: 7709–17.
- Busche MA, Eichhoff G, Adelsberger H, Abramowski D, Wiederhold KH, Haass C, et al. Clusters of hyperactive neurons near amyloid plaques in a mouse model of Alzheimer's disease. *Science* 2008; 321: 1686–9.
- Dale AM, Fischl B, Sereno MI. Cortical surface-based analysis: I. Segmentation and surface reconstruction. *Neuroimage* 1999; 9: 179–94.
- Desikan RS, Segonne F, Fischl B, Quinn BT, Dickerson BC, Blacker D, et al. An automated labeling system for subdividing the human cerebral cortex on MRI scans into gyral based regions of interest. *Neuroimage* 2006; 31: 968–80.
- Douaud G, Groves AR, Tamnes CK, Westlye LT, Duff EP, Engvig A, et al. A common brain network links development, aging, and vulnerability to disease. *Proc Natl Acad Sci USA* 2014; 111: 17648–53.
- Edison P, Archer HA, Hinz R, Hammers A, Pavese N, Tai YF, et al. Amyloid, hypometabolism, and cognition in Alzheimer disease: an [11C]PIB and [18F]FDG PET study. *Neurology* 2007; 68: 501–8.
- Elman JA, Madison CM, Baker SL, Vogel JW, Marks SM, Crowley S, et al. Effects of beta-amyloid on resting state functional connectivity within and between networks reflect known patterns of regional vulnerability. *Cereb Cortex* 2016; 26: 695–707.
- Fellin T, Pascual O, Gobbo S, Pozzan T, Haydon PG, Carmignoto G. Neuronal synchrony mediated by astrocytic glutamate through activation of extrasynaptic NMDA receptors. *Neuron* 2004; 43: 729–43.
- Fischl B, Liu A, Dale AM. Automated manifold surgery: constructing geometrically accurate and topologically correct models of the human cerebral cortex. *IEEE Trans Med Imaging* 2001; 20: 70–80.
- Fischl B, Salat DH, Busa E, Albert M, Dieterich M, Haselgrove C, et al. Whole brain segmentation: automated labeling of neuroanatomical structures in the human brain. *Neuron* 2002; 33: 341–55.
- Forster S, Grimmer T, Miederer I, Henriksen G, Yousefi BH, Graner P, et al. Regional expansion of hypometabolism in Alzheimer's disease follows amyloid deposition with temporal delay. *Biol Psychiatry* 2012; 71: 792–7.
- Greicius MD, Krasnow B, Reiss AL, Menon V. Functional connectivity in the resting brain: a network analysis of the default mode hypothesis. *Proc Natl Acad Sci USA* 2003; 100: 253–8.
- Hardy J, Selkoe DJ. The amyloid hypothesis of Alzheimer's disease: progress and problems on the road to therapeutics. *Science* 2002; 297: 353–6.
- Jack CR, Jr, Knopman DS, Jagust WJ, Shaw LM, Aisen PS, Weiner MW, et al. Hypothetical model of dynamic biomarkers of the Alzheimer's pathological cascade. *Lancet Neurol* 2010; 9: 119–28.
- Jack CR, Jr, Lowe VJ, Senjem ML, Weigand SD, Kemp BJ, Shiung MM, et al. 11C PiB and structural MRI provide complementary information in imaging of Alzheimer's disease and amnesic mild cognitive impairment. *Brain* 2008; 131: 665–80.
- Johnson SC, Christian BT, Okonkwo OC, Oh JM, Harding S, Xu G, et al. Amyloid burden and neural function in people at risk for Alzheimer's Disease. *Neurobiol Aging* 2014; 35: 576–84.
- Kalpourzos G, Chetelat G, Baron JC, Landeau B, Mevel K, Godeau C, et al. Voxel-based mapping of brain gray matter volume and glucose metabolism profiles in normal aging. *Neurobiol Aging* 2009; 30: 112–24.
- Khan UA, Liu L, Provenzano FA, Berman DE, Profaci CP, Sloan R, et al. Molecular drivers and cortical spread of lateral entorhinal cortex dysfunction in preclinical Alzheimer's disease. *Nat Neurosci* 2014; 17: 304–11.
- Klunk WE, Engler H, Nordberg A, Wang Y, Blomqvist G, Holt DP, et al. Imaging brain amyloid in Alzheimer's disease with Pittsburgh compound-B. *Ann Neurol* 2004; 55: 306–19.
- Knopman DS, Jack CR, Jr, Wiste HJ, Lundt ES, Weigand SD, Vemuri P, et al. F-fluorodeoxyglucose positron emission tomography, aging, and apolipoprotein E genotype in cognitively normal persons. *Neurobiol Aging* 2014; 35: 2096–106.
- Landau SM, Harvey D, Madison CM, Koeppe RA, Reiman EM, Foster NL, et al. Associations between cognitive, functional, and FDG-PET measures of decline in AD and MCI. *Neurobiol Aging* 2011; 32: 1207–18.
- Leech R, Kamourieh S, Beckmann CF, Sharp DJ. Fractionating the default mode network: distinct contributions of the ventral and dorsal posterior cingulate cortex to cognitive control. *J Neurosci* 2011; 31: 3217–24.
- Lehmann M, Madison CM, Ghosh PM, Seeley WW, Mormino E, Greicius MD, et al. Intrinsic connectivity networks in healthy subjects explain clinical variability in Alzheimer's disease. *Proc Natl Acad Sci USA* 2013; 110: 11606–11.
- Liang X, Zou Q, He Y, Yang Y. Coupling of functional connectivity and regional cerebral blood flow reveals a physiological basis for network hubs of the human brain. *Proc Natl Acad Sci USA* 2013; 110: 1929–34.
- Logan J, Fowler JS, Volkow ND, Wang GJ, Ding YS, Alexoff DL. Distribution volume ratios without blood sampling from graphical analysis of PET data. *J Cereb Blood Flow Metab* 1996; 16: 834–40.
- Lowe VJ, Weigand SD, Senjem ML, Vemuri P, Jordan L, Kantarci K, et al. Association of hypometabolism and amyloid levels in aging, normal subjects. *Neurology* 2014; 82: 1959–67.
- Mathis CA, Wang Y, Holt DP, Huang GF, Debnath ML, Klunk WE. Synthesis and evaluation of 11C-labeled 6-substituted 2-arylbenzothiazoles as amyloid imaging agents. *J Med Chem* 2003; 46: 2740–54.
- Meltzer CC, Kinahan PE, Greer PJ, Nichols TE, Comtat C, Cantwell MN, et al. Comparative evaluation of MR-based partial-volume correction schemes for PET. *J Nucl Med* 1999; 40: 2053–65.
- Mielke R, Kessler J, Szelies B, Herholz K, Wienhard K, Heiss WD. Normal and pathological aging—findings of positron-emission-tomography. *J Neural Transm* 1998; 105: 821–37.

- Minoshima S, Giordani B, Berent S, Frey KA, Foster NL, Kuhl DE. Metabolic reduction in the posterior cingulate cortex in very early Alzheimer's disease. *Ann Neurol* 1997; 42: 85–94.
- Mormino EC, Brandel MG, Madison CM, Marks S, Baker SL, Jagust WJ. Aβ deposition in aging is associated with increases in brain activation during successful memory encoding. *Cereb Cortex* 2012a; 22: 1813–23.
- Mormino EC, Brandel MG, Madison CM, Rabinovici GD, Marks S, Baker SL, et al. Not quite PIB-positive, not quite PIB-negative: slight PIB elevations in elderly normal control subjects are biologically relevant. *Neuroimage* 2012b; 59: 1152–60.
- Mosconi L. Brain glucose metabolism in the early and specific diagnosis of Alzheimer's disease. FDG-PET studies in MCI and AD. *Eur J Nucl Med Mol Imaging* 2005; 32: 486–510.
- Oh H, Habeck C, Madison C, Jagust W. Covarying alterations in Aβ deposition, glucose metabolism, and gray matter volume in cognitively normal elderly. *Hum Brain Mapp* 2014; 35: 297–308.
- Oh H, Madison C, Haight TJ, Markley C, Jagust WJ. Effects of age and beta-amyloid on cognitive changes in normal elderly people. *Neurobiol Aging* 2012; 33: 2746–55.
- Oh H, Mormino EC, Madison C, Hayenga A, Smiljic A, Jagust WJ. beta-Amyloid affects frontal and posterior brain networks in normal aging. *Neuroimage* 2011; 54: 1887–95.
- Ossenkoppele R, Madison C, Oh H, Wirth M, van Berckel BN, Jagust WJ. Is verbal episodic memory in elderly with amyloid deposits preserved through altered neuronal function? *Cereb Cortex* 2014; 24: 2210–18.
- Palop JJ, Mucke L. Amyloid-beta-induced neuronal dysfunction in Alzheimer's disease: from synapses toward neural networks. *Nat Neurosci* 2010; 13: 812–8.
- Pearson RC, Powell TP. The neuroanatomy of Alzheimer's disease. *Rev Neurosci* 1989; 2: 101–22.
- Price JC, Klunk WE, Lopresti BJ, Lu X, Hoge JA, Ziolkowski SK, et al. Kinetic modeling of amyloid binding in humans using PET imaging and Pittsburgh Compound-B. *J Cereb Blood Flow Metab* 2005; 25: 1528–47.
- Raichle ME, MacLeod AM, Snyder AZ, Powers WJ, Gusnard DA, Shulman GL. A default mode of brain function. *Proc Natl Acad Sci USA* 2001; 98: 676–82.
- Ranganath C, Ritchey M. Two cortical systems for memory-guided behaviour. *Nat Rev Neurosci* 2012; 13: 713–26.
- Roberson ED, Halabisky B, Yoo JW, Yao J, Chin J, Yan F, et al. Amyloid-beta/Fyn-induced synaptic, network, and cognitive impairments depend on tau levels in multiple mouse models of Alzheimer's disease. *J Neurosci* 2011; 31: 700–11.
- Segonne F, Dale AM, Busa E, Glessner M, Salat D, Hahn HK, et al. A hybrid approach to the skull stripping problem in MRI. *Neuroimage* 2004; 22: 1060–75.
- Sepulcre J, Sabuncu MR, Becker A, Sperling R, Johnson KA. In vivo characterization of the early states of the amyloid-beta network. *Brain* 2013; 136 (Pt 7): 2239–52.
- Shin J, Tsui W, Li Y, Lee SY, Kim SJ, Cho SJ, et al. Resting-state glucose metabolism level is associated with the regional pattern of amyloid pathology in Alzheimer's disease. *Int J Alzheimers Dis* 2011; 2011: 759780.
- Sorg C, Riedel V, Muhlau M, Calhoun VD, Eichele T, Laer L, et al. Selective changes of resting-state networks in individuals at risk for Alzheimer's disease. *Proc Natl Acad Sci USA* 2007; 104: 18760–5.
- Sperling RA, Laviolette PS, O'Keefe K, O'Brien J, Rentz DM, Pihlajamaki M, et al. Amyloid deposition is associated with impaired default network function in older persons without dementia. *Neuron* 2009; 63: 178–88.
- Spreng RN, Schacter DL. Default network modulation and large-scale network interactivity in healthy young and old adults. *Cereb Cortex* 2012; 22: 2610–21.
- Vaishnavi SN, Vlassenko AG, Rundle MM, Snyder AZ, Mintun MA, Raichle ME. Regional aerobic glycolysis in the human brain. *Proc Natl Acad Sci USA* 2010; 107: 17757–62.
- Vezzani A, Granata T. Brain inflammation in epilepsy: experimental and clinical evidence. *Epilepsia* 2005; 46: 1724–43.
- Vincent JL, Kahn I, Snyder AZ, Raichle ME, Buckner RL. Evidence for a frontoparietal control system revealed by intrinsic functional connectivity. *J Neurophysiol* 2008; 100: 3328–42.
- Vlassenko AG, Vaishnavi SN, Couture L, Sacco D, Shannon BJ, Mach RH, et al. Spatial correlation between brain aerobic glycolysis and amyloid-beta (Aβ) deposition. *Proc Natl Acad Sci USA* 2010; 107: 17763–7.
- Yan P, Bero AW, Cirrito JR, Xiao Q, Hu X, Wang Y, et al. Characterizing the appearance and growth of amyloid plaques in APP/PS1 mice. *J Neurosci* 2009; 29: 10706–14.